American Mineralogist, Volume 95, pages 699–705, 2010

The crystal structure of esperite, with a revised chemical formula, $PbCa_2(ZnSiO_4)_3$, isostructural with beryllonite

Kimberly T. Tait,[1,*] Hexiong Yang,[2] Robert T. Downs,[2] Chen Li,[2] and William W. Pinch[3]

[1]Department of Natural History, Royal Ontario Museum, 100 Queen's Park, Toronto, Ontario M5S 2C6, Canada
[2]Department of Geosciences, University of Arizona, Tucson, Arizona 85721-0077, U.S.A
[3]19 Stonebridge Lane, Pittsford, New York 14534, U.S.A.

Abstract

Esperite from Franklin, New Jersey, was first described by Moore and Ribbe (1965) as monoclinic with a well-developed "superlattice" $a = 2 \times 8.814(2)$ Å, $b = 8.270(3)$ Å, $c = 2 \times 15.26(1)$ Å, $\beta \approx 90°$, space group $P2_1/n$ (subcell), and the chemical formula $PbCa_3(ZnSiO_4)_4$. They attributed "superlattice" reflections to the ordered distributions of Pb and Ca cations over four beryllonite-type subcells for esperite with the Ca:Pb ratio greater than 2:1.

We examined two esperite fragments from the type sample using single-crystal X-ray diffraction, electron microprobe analysis, and Raman spectroscopy. Although both fragments have Ca:Pb ≈ 1.8, one exhibits the "superlattice" reflections as observed by Moore and Ribbe (1965), whereas the other does not. The sample without "superlattice" reflections has unit-cell parameters $a = 8.7889(2)$, $b = 8.2685(2)$, $c = 15.254(3)$ Å, $\beta = 90.050(1)°$, $V = 1108.49(4)$ Å^3, and the chemical composition $Pb_{1.00}(Ca_{1.86}Fe^{2+}_{0.07}Mn_{0.04}Cr^{3+}_{0.02})_{\Sigma=1.99}(Zn_{1.00}Si_{1.00}O_4)_3$. Its crystal structure was solved in space group $P2_1/n$ ($R_1 = 0.022$). Esperite is isostructural with beryllonite, $NaBePO_4$, and its ideal chemical formula should, therefore, be revised to $PbCa_2(ZnSiO_4)_3$, $Z = 4$. The ZnO_4 and SiO_4 tetrahedra in esperite share corners to form an ordered framework, with Pb^{2+} occupying the nine-coordinated site in the large channels and Ca^{2+} occupying the two distinct octahedral sites in the small channels. The so-called "superlattice" reflections are attributed to triple twins, a trilling of ~60° rotational twinning around the *b* axis, similar to those observed in many other beryllonite-type materials. A phase transformation from a high-temperature polymorph to the esperite structure is proposed to be responsible for the twinning formation.

Keywords: Esperite, beryllonite, Pb-Zn silicates, crystal chemistry, X-ray diffraction

Introduction

Two Pb-Zn silicate minerals, larsenite $PbZnSiO_4$ and "calcium-larsenite" $(Pb,Ca)ZnSiO_4$, from a metamorphosed stratiform zinc orebody in Franklin, New Jersey, were first described by Palache et al. (1928a, 1928b), who, based on morphological and chemical data, proposed that the two minerals were structurally related to olivine with orthorhombic symmetry. Subsequent X-ray diffraction studies by Layman (1957) and Moore and Ribbe (1965), however, revealed that neither of the two minerals is isomorphous with olivine. Furthermore, from various single-crystal X-ray diffraction photographs, Moore and Ribbe (1965) found that "calcium-larsenite" is also structurally different from larsenite, leading them to give the mineral a new name, esperite (also after Esper S. Larsen), with the ideal chemical formula $PbCa_3(ZnSiO_4)_4$. They described esperite as monoclinic with a well-developed superstructure: the subcell (excluding superlattice reflections) gives $a = 8.814$, $b = 8.270$, $c = 15.26$ Å, $\beta \approx 90°$, and space group $P2_1/n$, whereas the supercell (including superlattice reflections) is *B*-centered with doubled *a* (=2 × 8.814 Å) and *c* (=2 × 15.26 Å) dimensions. Intriguingly, without the structure determination, Moore and Ribbe (1965) noted that esperite might be structurally related to beryllonite $NaBePO_4$ or trimerite $CaMn^{2+}_2(BeSiO_4)_3$, but its chemical formula did not correspond. From X-ray diffraction experiments on both natural (from the type locality) and synthetic esperite specimens, Ito (1968) found that, unlike the natural sample, synthetic esperite displays no superlattice reflections and has a pseudo-orthorhombic cell with $a = 8.79$, $b = 8.29$, and $c = 15.25$ Å. Dunn (1985) conducted a series of electron microprobe analyses on Pb-silicates from Franklin, New Jersey, and concluded that the chemical composition of esperite varies principally in the Ca:Pb ratio, with an empirical formula $Ca_{2.80}Pb_{1.15}Mn_{0.08}Mg_{0.09}Zn_{3.80}Si_{4.04}O_{16}$. To date, esperite has only been reported from one other locality, the El Dragón mine, Potosi, Bolivia (Grundmann et al. 1990), but no chemical composition has been given for that occurrence. Since then, no detailed crystallographic study on esperite has been reported. In this paper, we report the results of our re-examination of esperite from the holotype sample by means of single-crystal X-ray diffraction, electron microprobe analysis, and Raman spectroscopy and re-define its ideal chemical formula as $PbCa_2(ZnSiO_4)_3$, based on our determined structure model.

Experimental methods

A fragment of esperite from the holotype sample [CMNMC 56855 in the Canadian Museum of Nature Mineral Collection in Ottawa, originally studied by Moore and Ribbe (1965)], Parker Shaft, Franklin, Sussex Co., New Jersey, U.S.A., was obtained for this study, which is now in the collection of the RRUFF project

* E-mail: ktait@rom.on.ca

(deposition no. R070512; http://rruff.info/R070512). Based on optical examination and X-ray diffraction peak profiles, two nearly equi-dimensional single crystals, sample 1 with dimensions 0.05 × 0.05 × 0.06 mm and sample 2 with dimensions 0.07 × 0.06 × 0.06 mm, were selected for the experiments. X-ray diffraction data were collected on a Bruker X8 APEX2 CCD X-ray diffractometer using graphite-monochromatized Mo$K\alpha$ radiation. Detailed procedures for data collections and processes were similar to those described by Yang and Downs (2008). To our surprise, the two selected crystals yielded different outcomes: The unit-cell dimensions of samples 1 and 2 correspond, respectively, to those for the subcell and supercell reported by Moore and Ribbe (1965) (Fig. 1). Further analysis demonstrated that the pseudo-hexagonal unit-cell dimensions of sample 2 are actually a result of triple twins corresponding to a ~60 rotation around the *b* axis of the monoclinic cell (Fig. 2). If we use $\boldsymbol{a}_H$, $\boldsymbol{b}_H$, and $\boldsymbol{c}_H$ to represent the pseudo-hexagonal cell (or "supercell") parameters, $\boldsymbol{a}_1$, $\boldsymbol{b}_1$, and $\boldsymbol{c}_1$ for monoclinic cell 1, $\boldsymbol{a}_2$, $\boldsymbol{b}_2$, and $\boldsymbol{c}_2$ for monoclinic cell 2, and $\boldsymbol{a}_3$, $\boldsymbol{b}_3$, and $\boldsymbol{c}_3$ for monoclinic cell 3, then the transformation from the pseudo-hexagonal cell to monoclinic cell 1 is

$$\begin{bmatrix} a_1 \\ b_1 \\ c_1 \end{bmatrix} = \begin{pmatrix} 0.5 & 0 & 0 \\ 0 & 0 & 1 \\ 0.5 & 1 & 0 \end{pmatrix} \begin{bmatrix} a_H \\ b_H \\ c_H \end{bmatrix}.$$

The matrix for the transformation from monoclinic cell 1 to 2 is

$$\begin{pmatrix} 0.5 & 0 & 0.5 \\ 0 & 1 & 0 \\ -1.5 & 0 & 0.5 \end{pmatrix}$$

and that for the transformation from monoclinic cell 1 to 3 is

$$\begin{pmatrix} -0.5 & 0 & 0.5 \\ 0 & 1 & 0 \\ -1.5 & 0 & -0.5 \end{pmatrix}.$$

Subsequently, the X-ray intensity data of sample 2 were processed with the software TWINABS (Sheldrick 2007). All reflections of both samples were indexed on the basis of a monoclinic unit cell. The systematic absences of reflections point to the unique space group $P2_1/n$. The structures of both esperite crystals were solved and refined using SHELXL97 (Sheldrick 2008). Though the two samples produced rather comparable structural data, only the results from sample 1 are given here because of its better refinement statistics (e.g., $R_1 = 0.022$ for sample 1 vs. 0.047 for sample 2). The effects of including the trace amounts of Fe, Mn, and Cr on the crystal structure were tested in the refinements and they were found to be insignificant, so the crystal chemistry was assumed to be ideal, $PbCa_2(ZnSiO_4)_4$, throughout the structure refinements. Final crystallographic and refinement statistics data are listed in Table 1, atomic coordinates and isotropic displacement parameters in Table 2, anisotropic displacement parameters in Table 3, and selected interatomic distances in Table 4. (CIF[1] is on deposit.)

The chemical compositions of the two crystals examined by X-ray diffraction were analyzed with a Cameca SX50 electron microprobe with an accelerating potential of 15 kV and a beam current of 20 nA. Standards included diopside for Si and Ca, rhodonite for Mn, wulfenite for Pb, fayalite for Fe, chromite for Cr, and willemite for Zn. Online reduction of the raw data was done using the ZAF matrix correction. The average results (eight analysis points for each sample) are given Table 5.

The Raman spectrum of esperite was collected from a randomly oriented crystal at 100% power on a Thermo Almega microRaman system, using a solid-state laser with a frequency of 780 nm, and a thermoelectrically cooled CCD detector. The laser is partially polarized with 4 cm^{-1} resolution and a spot size of 1 μm. The Raman spectra of the two esperite crystals used for the X-ray diffraction experiments are essentially indiscernible.

[1] Deposit item AM-10-026, CIF. Deposit items are available two ways: For a paper copy contact the Business Office of the Mineralogical Society of America (see inside front cover of recent issue) for price information. For an electronic copy visit the MSA web site at http://www.minsocam.org, go to the *American Mineralogist* Contents, find the table of contents for the specific volume/issue wanted, and then click on the deposit link there.

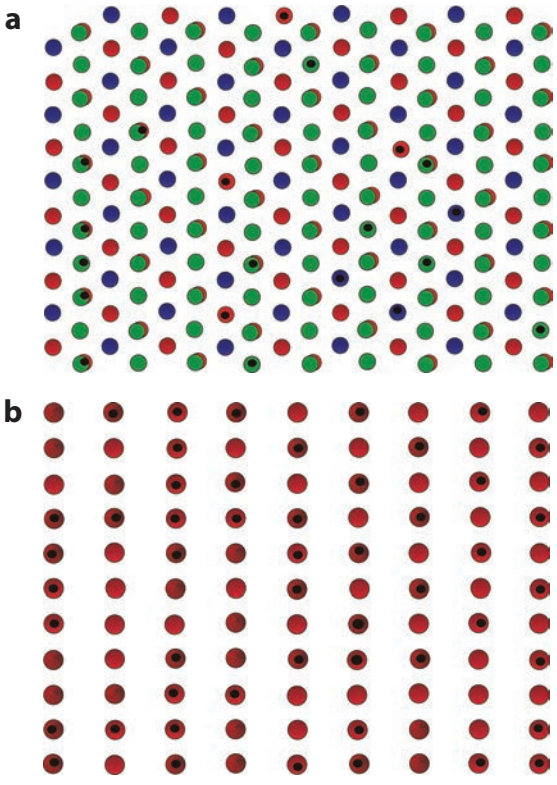

FIGURE 1. Reciprocal plots of X-ray reflections (viewed down **b***) from (**a**) twinned and (**b**) untwinned esperite samples. The blue, green, and red spheres in **a** represent reflections from three different twin domains, whereas the small black spheres in **b** represent weak reflections [$I < 5\sigma(I)$].

DISCUSSION

Crystal structure

Esperite is isotypic with beryllonite, $NaBePO_4$ (Golovastikov 1961; Giuseppetti and Tadini 1973), a stuffed derivative of tridymite. Materials belonging to the large family of tridymite derivatives have been of growing interest owing to their structural properties, such as the open-framework architecture and polymorphism, as well as their physical properties, including ferroic properties or potential as hosts for fluorescent materials (e.g., Hammond et al. 1998). A review on the structural behavior of tetrahedral framework compounds as a function of temperature, pressure, and composition has been presented by Taylor (1983, 1984). In addition to esperite, many other compounds exhibit the beryllonite-type structure, such as trimerite $CaMn_2^{2+}(BeSiO_4)_3$ (Aminoff 1926; Klaska and Jarchow 1977), synthetic $NaBSiO_4$ (Graetsch and Schreyer 2005), $NaAlGeO_4$ (Sandomirskii et al. 1986; Barbier and Fleet 1987, 1988; Chen et al. 1994), $NaGaSiO_4$ (Barbier and Fleet 1987; Chen et al. 1994), $NaGaGeO_4$ (Barbier and Fleet 1987), $KAlGeO_4$, $KGaSiO_4$, $KGaGeO_4$ (Barbier and Fleet 1987), $CaAl_2O_4$ (Hörkner and Müller-Buschbaum 1976), $CaAl_{1.8}Fe_{0.2}O_4$ (Kahlenberg 2001), $AgXPO_4$ (X = Be, Zn) (Hammond et al. 1998), and $BaZnGeO_4$ (Iijima et al. 1982). Another closely related mineral is malinkoite $NaBSiO_4$ (Sokolova et al. 2001), which has a synthetic polymorph that is isostructural with beryllonite (Graetsch and Schreyer 2005).

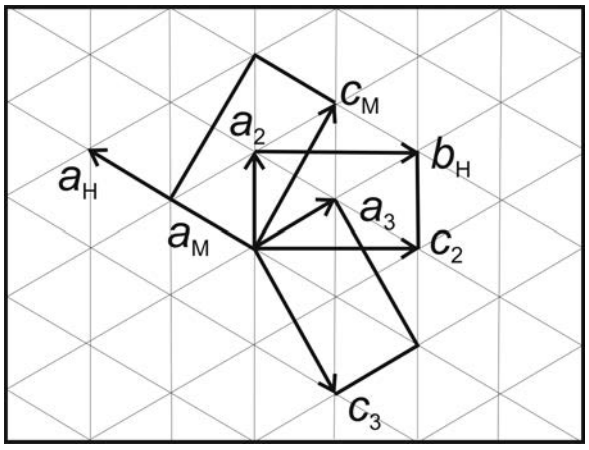

FIGURE 2. Illustration of triple twins, viewed along the *b* axis of the esperite cell, and their relationships with the pseudo-hexagonal cell. The *a* and *b* dimensions of the pseudo-hexagonal cell are indicated by a_H and b_H, respectively. The three monoclinic esperite cells, indicated by a_1 and c_1 for cell 1, a_2 and c_2 for cell 2, and a_3 and c_3 for cell 3, are related by a trilling of ~60° rotational twinning around the *b* axis.

TABLE 1. Crystallographic and refinement statistics data for esperite

Ideal chemical formula	$PbCa_2(ZnSiO_4)_3$
a (Å)	8.7889(2)
b (Å)	8.2685(2)
c (Å)	15.2535(3)
β (°)	90.050(1)
V (Å^3)	1108.49(4)
Space group	$P2_1/n$ (no. 14)
Z	4
μ (mm^{-1})	22.96
D(calc) (g/cm^3)	4.564
θ range for data collection (°)	2.67–40.81
Reflections collected	24487
Unique reflections	7025
$I > 2\sigma(I)$	5935
Parameters refined	191
R(int) (%)	3.21
R (%) [$I > 2\sigma(I)$]	R_1 = 2.22 and wR2 = 4.41
R (%) (all data)	R_1 = 3.07 and wR2 = 4.61
Goodness of fit	1.001

In tridymite and its stuffed derivatives, corner-sharing of the tetrahedra results in a three dimensional framework in which the tetrahedra form layers made up of six-membered rings [see reviews by Taylor (1983, 1984)]. Various derivatives of tridymite differ chiefly in the stacking of tetrahedral layers and the configurations of six-membered rings. In tridymite, nepheline, and kalsilite, there is only one type of six-membered ring of tetrahedra, with apices that point alternately up (U) and down (D), when viewed along the hexagonal or pseudo-hexagonal axis. In the beryllonite-type materials, however, only a third of the rings are of the UDUDUD type, whereas two thirds of the rings are of the UUDDUD type. The general chemical formula for beryllonite-type materials can be expressed as $AYXO_4$ or $AB_2(YXO_4)_3$, where *X* and *Y* are the tetrahedral framework formers and *A* and/or *B* are the framework modifiers. In the esperite structure, the three-dimensional framework consists of the corner-shared ZnO_4 and SiO_4 tetrahedra, with the UDUDUD and UUDDUD rings encapsulating two distinct channels that run parallel to the *b* axis (Fig. 3a). The channels made of the

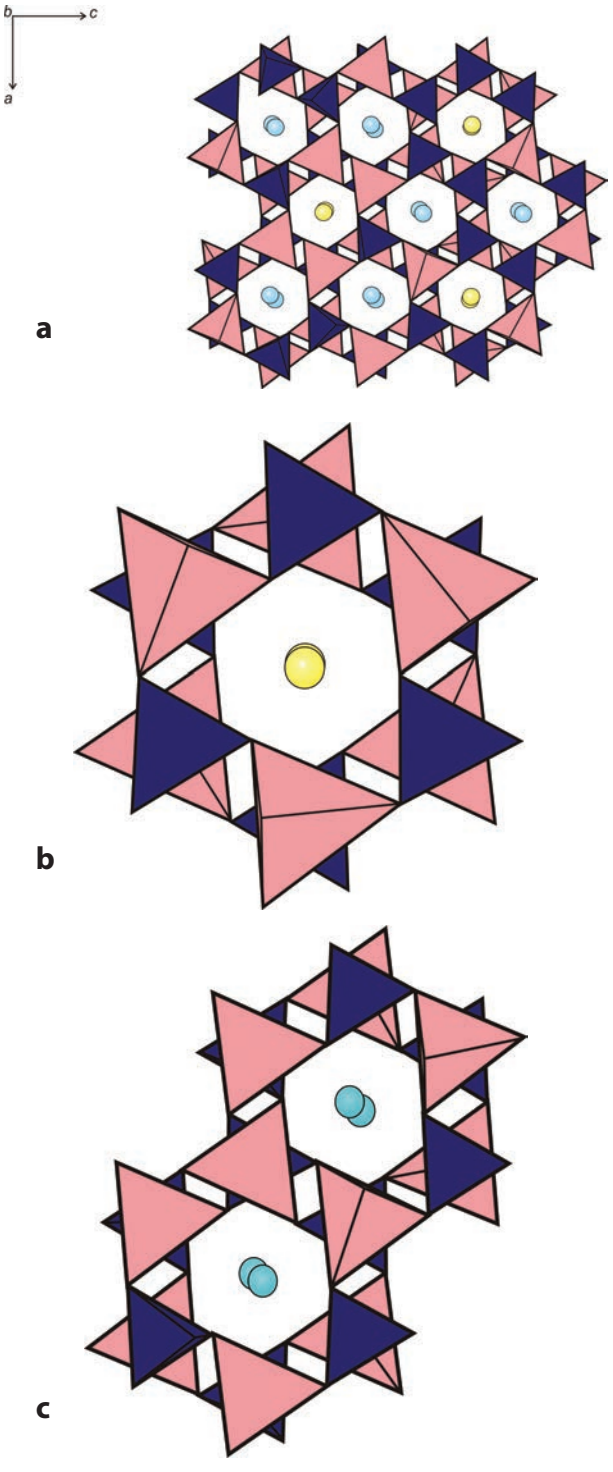

FIGURE 3. (**a**) The tetrahedral framework of the esperite structure viewed down the *b* axis. The SiO_4 and ZnO_4 tetrahedra are colored dark blue and pink, respectively. There are two types of rings in the esperite structure: (**b**) the larger UDUDUD rings and (**c**) the smaller UUDDUD rings, where U and D represent apices of tetrahedra pointing up and down, respectively. There are twice as many UUDDUD rings as UDUDUD rings, which are occupied by Ca^{2+} (turquoise spheres) and Pb^{2+} (yellow spheres) cations, respectively.

TABLE 2. Coordinates and isotropic displacement parameters of atoms in esperite

	x	*y*	*z*	U_{iso}
Pb	0.245756(8)	0.055200(9)	0.250826(5)	0.00928(2)
Ca1	0.73827(4)	0.46078(5)	0.07414(3)	0.00779(6)
Ca2	0.76071(4)	0.03835(5)	0.08855(3)	0.00768(6)
Zn1	0.57626(3)	0.33526(3)	0.24338(2)	0.00795(4)
Zn2	0.07422(3)	0.33879(3)	0.09038(2)	0.00789(4)
Zn3	0.09274(3)	0.33936(3)	0.41626(2)	0.00797(4)
Si1	0.91112(6)	0.22833(7)	0.26527(4)	0.00588(9)
Si2	0.43933(6)	0.22969(7)	0.41207(4)	0.00581(9)
Si3	0.39507(6)	0.22585(7)	0.07455(4)	0.00596(9)
O1	0.4095(2)	0.2295(2)	0.1819(1)	0.0094(2)
O2	0.4339(2)	0.7366(2)	0.2947(1)	0.0093(2)
O3	0.2698(2)	0.2303(2)	0.3661(1)	0.0095(2)
O4	0.7684(2)	0.2503(2)	0.1979(1)	0.0087(2)
O5	0.9125(2)	0.2422(2)	0.0170(1)	0.0082(2)
O6	0.5655(2)	0.2541(2)	0.0346(1)	0.0086(2)
O7	0.5464(2)	0.3672(2)	0.3678(1)	0.0097(2)
O8	0.2762(2)	0.3633(2)	0.0417(1)	0.0099(2)
O9	0.9147(2)	0.3644(2)	0.3420(1)	0.0097(2)
O10	0.5889(2)	0.5519(2)	0.1881(1)	0.0115(3)
O11	−0.0172(2)	0.5545(2)	0.1060(1)	0.0102(3)
O12	0.1723(2)	0.5508(2)	0.4532(1)	0.0103(3)

TABLE 3. Anisotropic displacement parameters of atoms in esperite

Atom	U_{11}	U_{22}	U_{33}	U_{12}	U_{13}	U_{23}
Pb	0.01076(3)	0.00671(3)	0.01038(3)	0.00027(2)	0.00008(2)	−0.00001(2)
Ca1	0.0082(2)	0.0068(2)	0.0084(2)	−0.0006(1)	0.0008(1)	0.0004(1)
Ca2	0.0095(2)	0.0060(2)	0.0076(2)	−0.0006(1)	−0.0010(1)	0.0004(1)
Zn1	0.00805(9)	0.00877(9)	0.00704(9)	−0.00053(7)	0.00070(7)	−0.00056(7)
Zn2	0.00759(9)	0.00824(9)	0.00786(9)	−0.00036(7)	0.00004(7)	0.00054(7)
Zn3	0.00828(9)	0.00850(9)	0.00713(9)	0.00048(7)	−0.00057(7)	−0.00032(7)
Si1	0.0062(2)	0.0058(2)	0.0057(2)	0.0005(2)	−0.0001(2)	−0.0003(2)
Si2	0.0062(2)	0.0059(2)	0.0053(2)	−0.0003(2)	0.0005(2)	0.0000(2)
Si3	0.0060(2)	0.0058(2)	0.0062(2)	−0.0005(2)	0.0002(2)	0.0001(2)
O1	0.0095(6)	0.0121(6)	0.0066(6)	−0.0038(5)	0.0005(5)	−0.0003(5)
O2	0.0075(6)	0.0121(6)	0.0083(6)	−0.0016(5)	0.0007(5)	−0.0038(5)
O3	0.0079(6)	0.0117(6)	0.0089(6)	0.0023(5)	−0.0019(5)	−0.0038(5)
O4	0.0080(6)	0.0109(6)	0.0071(6)	0.0019(5)	−0.0012(4)	−0.0016(5)
O5	0.0097(6)	0.0096(6)	0.0052(5)	−0.0020(5)	0.0004(4)	−0.0002(4)
O6	0.0067(6)	0.0104(6)	0.0088(6)	−0.0015(5)	0.0012(4)	−0.0018(5)
O7	0.0130(6)	0.0088(6)	0.0073(6)	−0.0034(5)	0.0019(5)	0.0002(4)
O8	0.0091(6)	0.0087(6)	0.0118(6)	0.0021(5)	0.0013(5)	0.0041(5)
O9	0.0107(6)	0.0085(6)	0.0098(6)	0.0015(5)	−0.0029(5)	−0.0036(5)
O10	0.0173(7)	0.0063(6)	0.0108(6)	−0.0007(5)	0.0033(5)	−0.0009(5)
O11	0.0096(6)	0.0055(6)	0.0156(7)	−0.0006(4)	0.0012(5)	0.0004(5)
O12	0.0123(6)	0.0067(6)	0.0120(6)	0.0011(5)	−0.0034(5)	0.0005(5)

TABLE 4. Selected interatomic distances in esperite

Pb-O1	2.293(1)	Si1-O2	1.643(2)
Pb-O1	3.189(2)	Si1-O4	1.631(2)
Pb-O2	2.286(1)	Si1-O9	1.624(2)
Pb-O2	3.182(2)	Si1-O10	1.623(2)
Pb-O3	2.288(1)	<Si1-O>	1.630
Pb-O3	3.228(2)		
Pb-O10	3.086(2)	Si2-O3	1.646(2)
Pb-O11	3.233(2)	Si2-O5	1.635(2)
Pb-O12	3.196(2)	Si2-O7	1.623(2)
	2.887	Si2-O11	1.626(2)
		<Si2-O>	1.632
Ca1-O4	2.581(2)		
Ca1-O5	2.524(2)	Si3-O1	1.643(1)
Ca1-O6	2.364(2)	Si3-O6	1.634(2)
Ca1-O8	2.292(2)	Si3-O8	1.622(2)
Ca1-O10	2.306(2)	Si3-O12	1.620(2)
Ca1-O11	2.335(2)	<Si3-O>	1.63
<Ca1-O>	2.401		
		Zn1-O1	1.947(2)
Ca2-O4	2.421(2)	Zn1-O4	1.957(1)
Ca2-O5	2.411(1)	Zn1-O7	1.934(1)
Ca2-O6	2.608(2)	Zn1-O10	1.983(1)
Ca2-O7	2.306(2)	<Zn1-O>	1.955
Ca2-O9	2.360(1)		
Ca2-O12	2.325(2)	Zn2-O2	1.947(1)
<Ca2-O>	2.405	Zn2-O5	1.977(1)
		Zn2-O8	1.936(1)
		Zn2-O11	1.971(1)
		<Zn2-O>	1.958
		Zn3-O3	1.955(1)
		Zn3-O6	1.978(1)
		Zn3-O9	1.942(2)
		Zn3-O12	1.965(1)
		<Zn3-O>	1.96

TABLE 5. Chemical composition of esperite

Oxide (wt%)	1	2	3	4	5	6
ZnO	31.47	31.07	30.61	32.3	34.5	
PbO	29.55	29.12	27.63	26.8	26.1	
SiO_2	23.83	23.76	24.10	25.3	27.1	
CaO	13.53	13.18	16.36	16.4	14.3	
FeO_{tot}	0.70	1.24	0.48			
MnO	0.33	0.33	0.57	0.6		
MgO			0.23	0.4		
Cr_2O_3	0.20	0.44				
Total	99.62	99.14	99.98	101.8	102.0	
Cation numbers normalized based on 12 O atoms						
Ca	1.86	1.79	2.18	2.11	1.80	2.07
Fe	0.07	0.13	0.05	0.00		
Mn	0.04	0.04	0.06	0.06		
Cr	0.02	0.04	0.00	0.00		
Σ	1.99	2.00	2.29	2.17	1.80	2.07
Pb	1.00	0.99	0.92	0.87	0.83	0.93
Zn	3.00	3.00	2.81	2.86	3.00	3.00
Si	3.00	3.00	2.99	3.01	3.19	3.00

Notes: 1 and 2 = samples 1 and 2 of this study, respectively; 3 = Palache et al. (1928); 4 = Dunn (1985). 5 = Ito (1968), natural sample; 6 = Ito (1968), synthetic sample. No values for weight percentage were given.

UDUDUD rings (Fig. 3b) are larger than those made of the UUDDUD rings (Fig. 3c), which are hereafter abbreviated as L- and S-channels, respectively, for simplicity. The S-channels contain two nonequivalent, face-sharing CaO_6 octahedral sites (Ca1 and Ca2), with the Ca-Ca distances alternating as 3.505 and 4.785 Å, whereas the L-channels contain the nine-coordinated Pb cations, with a Pb-Pb separation of 4.135 Å.

The two distinct CaO_6 octahedra display a similar average <Ca-O> distance of ~2.40 Å, with individual bond lengths ranging between 2.3 and 2.6 Å. As is typical for face-sharing polyhedra, the bonds associated with the three face-shared O atoms, O4, O5, O6, are longer than the rest of the Ca-O bonds within the distorted CaO_6 octahedra. The Pb cation is situated in a nine-coordinated, highly distorted tricapped trigonal antiprism, with an average <Pb-O> distance of 2.887 Å. However, the individual Pb-O bond lengths vary remarkably: While the Pb-O1, Pb-O2, and Pb-O3 bond distances are only ~2.29 Å, the other six Pb-O bonds are greater than 3.0 Å, indicating that Pb is considerably off-centered. In fact, the three short Pb-O bond distances in esperite are even shorter than the shortest Ca-O bonds (Table 4). They are also shorter than the corresponding Ca-O bond lengths (~2.388 Å) in isostructural $CaAl_2O_4$ and $CaAl_{1.8}Fe_{0.2}O_4$ (Kahlenberg 2001), despite the larger ionic radius of Pb^{2+} (1.35 vs. 1.18 Å for Ca^{2+} in the nine-coordination). By comparing $SrAl_2O_4$ and $BaAl_2O_4$ with $CaAl_2O_4$ and $CaAl_{1.8}Fe_{0.2}O_4$, Kahlenberg (2001) suggested that the magnitude of the coordination distortion of cations in the channels formed by the UDUDUD rings increases with decreasing cation radius, and Ca^{2+} shows the worst adaptation to such an environment and is ~33% under-bonded with regard to the ideal valence value of 2. Our data apparently contradict this statement. Moreover, the calculation of bond-valence sums

using the parameters given by Brese and O'Keeffe (1991) shows that Pb^{2+} in esperite is actually slightly over-bonded (2.192 v.u.) due to its pronounced "one-sided" coordination. The calculated bond valences for the three short Pb-O bonds sum to 1.861 v.u., making up 85% of its total bond valence. It should be pointed out that the one-sided coordination for Pb^{2+} we report here has also been observed in litharge and massicot (dimorphs of PbO), as well as in several other complex lead salts (e.g., Sahl 1970; Abel 1973; Hill 1985).

The strongly under-bonded nature of Ca^{2+} in the L-channels in beryllonite-type $CaAl_2O_4$ and $CaAl_{1.8}Fe_{0.2}O_4$ (Kahlenberg 2001) indicates that there is a geometrical mismatch between the Ca^{2+} size and the topology of the UDUDUD rings, which could potentially lower the stability of these two phases and make this site a possible target of attack by water (Kahlenberg 2001). Accordingly, accommodation of Ca^{2+} by the nine-coordinated site in the L-channels in beryllonite-type materials should be energetically unfavorable and avoided. For esperite, however, this site may be able to accommodate a certain amount of Ca^{2+}, owing to its over-bonded nature when it is fully occupied by Pb^{2+}. For the same reason, we think that the Pb^{2+} substitution for Ca^{2+} in the six-coordinated sites in the S-channels in esperite is probably very limited, as both Ca1 and Ca2 are only slightly under-bonded, with bond-valence sums of 1.936 and 1.899 v.u., respectively. In other words, it is not the short face-sharing contact between the Ca1 and Ca2 sites (3.505 Å) that precludes the accommodation of Pb^{2+} in the S-channels, since short Pb-Pb distances (~3.5 Å) have been found in Pb-metal and in the channels of lead aluminosilicate hollandite (Downs et al. 1995). Instead, it is most likely to result from the bonding requirements of the cations in the two sites. Similar arguments have also been given by Taylor (1983, 1984) and Barbier and Fleet (1987) for other tetrahedral framework materials.

Chemical formula of esperite

Given the determined structure, the chemical formula of esperite should therefore be revised based on 12 O atoms, rather than on 16, as previously suggested (Moore and Ribbe 1965; Dunn 1985). Accordingly, for our sample 1, we have a chemical formula of $Pb_{1.00}(Ca_{1.86}Fe^{2+}_{0.07}Mn_{0.04}Cr^{3+}_{0.02})_{\Sigma=1.99}(Zn_{1.00}Si_{1.00}O_4)_3$, or ideally $PbCa_2(ZnSiO_4)_3$. Recasting the chemical data reported by Palache et al. (1928a) and Dunn (1985) for esperite (Table 5) based on 12 O atoms yields $(Pb_{0.92}Ca_{0.08})_{\Sigma=1}Ca_{2.10}(Zn_{2.81}Mn_{0.06}Fe_{0.05})_{\Sigma=2.92}Si_{2.99}O_{12}$ (assuming tetrahedral Mn and Fe) and $(Pb_{0.87}Ca_{0.11})_{\Sigma=0.98}Ca_{2.00}(Zn_{2.86}Mn_{0.06})_{\Sigma=2.92}Si_{3.01}O_{12}$ (assuming tetrahedral Mn), respectively.

The Ca:Pb and Si:Zn ratios are noticeably different in all examined esperite samples from the type locality (Table 5). These two ratios are 2.35:1 and 1.07:1, respectively, as given by Palache (1935), and 2.43:1 and 1.06:1 by Dunn (1985). Though Moore and Ribbe (1965) did not report the detailed chemistry of their esperite sample, they stated that the Ca:Pb and Si:Zn ratios "are very close to 3:1 and 1:1, respectively." To establish a relationship between esperite and larsenite, Ito (1968) synthesized a series of Pb-Zn-Ca silicates with the general formula $Pb_xCa_yZn_zSiO_{2+n}$ ($n = x + y + z$; $x < 2$; $y \le 1$; $z \le 2$), which include larsenite $PbZnSiO_4$, barysilite $(Pb,Mn)_3Si_2O_7$, esperite $(Ca_{0.69}Pb_{0.31})_4Zn_4Si_4O_{16}$, margarosanite $Ca_2PbSi_3O_9$, phase X_1 $Pb_2CaZn_3Si_3O_{12}$, phase X_2 (possibly a high-temperature polymorph of nasonite $Ca_2Pb_3Si_3O_{11}$), and phase X_3 (probable formula $CaZnSi_2O_6{\cdot}H_2O$). However, he was unable to obtain esperite with the Ca:Pb ratio of 3:1 as suggested by Moore and Ribbe (1965) because there was always a small amount of other phases coexisting with esperite, such as phase X_1 and hardystonite $Ca_2ZnSi_2O_7$. Nonetheless, if we recast the chemical data for esperite synthesized by Ito (1968) on the basis of 12 O atoms, then we have a chemical formula of $Pb_{0.93}Ca_{2.07}(ZnSiO_4)_3$, which is obviously very close to the ideal formula we proposed above. Interestingly, the chemistry of synthetic phase X_1 (Ito 1968), $Pb_2Ca(ZnSiO_4)_3$, is very similar to that of esperite, $PbCa_2(ZnSiO_4)_3$, except for the Ca:Pb ratio, implying that this phase may be a tetrahedral framework material as well. The distinct powder X-ray diffraction patterns of the two phases (Ito 1968) point to an incomplete solid solution between them. By analogy with $KNa_2(AlGeO_4)_3$ (the beryllonite-type structure) and $K_2Na(AlGeO_4)_3$ (hexagonal kalsilite-type structure) (Klaska et al. 1979; Barbier and Fleet 1988), we postulate that phase X_1 may be isostructural with or topologically similar to kalsilite.

Raman spectroscopic data

There have been numerous investigations on various tetrahedral framework compounds (e.g., silica, feldspars, sodalites, zeolites, etc.) with Raman spectroscopy. Nevertheless, there is no Raman spectroscopic study on beryllonite-type materials in the literature. Plotted in Figure 4 is the Raman spectrum of esperite, along with that of beryllonite (taken from the RRUFF project: R060299) for comparison. The Raman spectra of both esperite and beryllonite can be tentatively classified into four regions. Region 1 includes the bands between 800 and 1100 cm^{-1}, which are assigned to *X*-O stretching vibrations within the strongly bonded XO_4 tetrahedra. These bands are characteristic of tetrahedral frameworks (e.g., Swainson et al. 2003; Zhang et al. 2003; Kihara et al. 2005; Khavryuchenko et al. 2007). The bands in region 2, between ~470 and 650 cm^{-1}, are attributed to the *X*-O-*Y* bending vibrations. In region 3, from 320 to 470 cm^{-1}, the bands are associated mainly with *Y*-O stretching vibrations within the more weakly bonded YO_4 tetrahedra. The bands

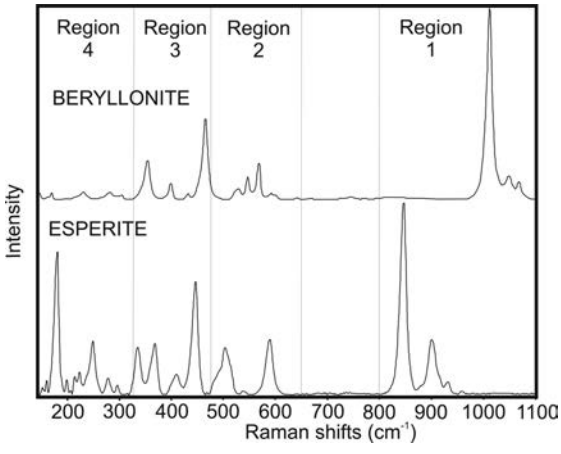

FIGURE 4. Raman spectrum of esperite, along with that of beryllonite for comparison.

in region 4, which span from 50 to 320 cm^{-1}, are of complex nature, primarily due to lattice modes involving *A*-O (and/or *B*-O) interactions, as well as *X*-O-*Y* bending and tetrahedral (XO_4 and YO_4) librations. Specifically, for the Raman spectrum of esperite, the strong, narrow band at 846 cm^{-1} in region 1 is assigned to the Si-O symmetric stretching vibrations within the SiO_4 group and three weak peaks at 900, 931, and 958 cm^{-1} to asymmetric stretching of Si-O bonds. There are three major Si-O-Zn bending modes at 504, 538, and 589 cm^{-1} in region 2. The bands in region 3 are characterized by a Zn-O symmetric stretching mode at 447 cm^{-1}, and three asymmetric stretching modes at 335, 368, and 409 cm^{-1}.

Origin of "superlattice" reflections in esperite

Based on the striking similarities in X-ray diffraction patterns between esperite and beryllonite, Moore and Ribbe (1965), without solving the esperite structure, proposed a Ca-Pb ordering scheme to account for the observed "superlattice" reflections in esperite, by assuming that Ca in excess of 2 apfu will have to enter the L-channels. They described such ordering in esperite in terms of four beryllonite-like subcells with Pb substituted in the larger, nine-coordinated Na1 site in each subcell, and (Ca+Pb) in the Na1 site of the immediately adjacent subcells. The Ca cations are substituted in the smaller, octahedrally coordinated Na2 or Na3 sites of the beryllonite structure. The alternate subcells are of different compositions, thus resulting in the superlattice reflections. This ordering model predicts no superstructure for esperite with the Ca:Pb ratio smaller than 2:1, since all Ca cations can be accommodated into the smaller sites in the S-channels, and none will enter the larger sites in the L-channels. Evidently, this is not the case for our samples because the two crystals we examined both have Ca:Pb ratios smaller than 2:1, with 1.86:1 for sample 1 and 1.79:1 for sample 2 (Table 5). Yet, sample 2 exhibits the "superlattice" reflections as Moore and Ribbe (1965) described, but sample 1 does not, indicating that cation ordering is not the cause of "superlattice" reflections in esperite.

A survey of materials with the beryllonite-type structure reveals that many of them have been found to display "superlattice" reflections similar to those observed by Moore and Ribbe (1965), such as trimerite (Aminoff 1926; Klaska and Jarchow 1977), (K,Na)$GaGeO_4$ (Barbier and Fleet 1987), (K,Na)$AlGeO_4$ (Barbier and Fleet 1988), Ba*M*SiO_4 (*M* = Co, Zn, Mg) (Liu and Barbier 1993), and Na(Al,Ga)SiO_4 (Chen et al. 1994). In all these cases, the "superlattice" reflections, which give rise to a marked orthohexagonal or pseudo-hexagonal character, are attributed to the presence of triple twins, often called trillings (drillings in German, e.g., Sheldrick 1997). In fact, the crystal structure of trimerite was solved from triply twinned data (Klaska and Jarchow 1977).

Barbier and Fleet (1988), in their investigation of phase relations in the (Na,K)$AlGeO_4$ system over a temperature range of 700–1100 °C, found four distinct structure types, including the beryllonite-, nepheline-, kalsilite-, and $KAlGeO_4$-types in order of increasing $KAlGeO_4$ content. Most interesting to note is that the diffraction pattern for the $NaAlGeO_4$ phase quenched from 1100 °C is "somewhat different from that of the beryllonite phase (stable below 900 °C)," showing a pronounced pseudo-hexagonal character. Barbier and Fleet (1988) ascribed this pseudo-hexagonal symmetry to triple twins on the basis of their TEM observations. Although the structure of the high-temperature form of $NaAlGeO_4$ was undetermined, Barbier and Fleet (1988) demonstrated that the transformation between the low- and high-temperature phases is completely reversible between 900 and 1100 °C. A similar reversible transition (from a high-temperature hexagonal phase to a low-temperature form of lower symmetry) has also been reported by Henderson and Roux (1977) in the (Na,K)$AlSiO_4$ system. This then begs the question about the formation mechanism of triple twins in beryllonite-type materials—does it originate from a growth morphology due to the pseudo-hexagonal character of these compounds or from a hexagonal-to-monoclinic transformation as a consequence of changing temperature or chemical compositions? More detailed research is apparently needed on beryllonite-type materials as a function of temperature and composition to address this question. As for $NaAlGeO_4$, because the material synthesized below 900 °C does not show "superlattice" reflections, but that quenched from 1100 °C does (Barbier and Fleet 1988), we propose that the twinning in $NaAlGeO_4$ is most likely to result from the structural transformation from a high-temperature form to the beryllonite-type structure. By the same token, we think that the twinning in esperite also stems from a phase transformation, since the crystals synthesized between 550 and 680 °C do not exhibit "superlattice" reflections (Ito 1968), but natural materials do (Moore and Ribbe 1965; Ito 1968), including our sample 2. In other words, we propose that there exists an unquenchable high-temperature form of esperite, which, according to the phase diagram determined by Ito (1968), will convert to $P2_1/n$ esperite below 680 °C. Indeed, the high-temperature X-ray diffraction experiment by Moore and Ribbe (1965) lends strong support to our inference, because they detected a phase transformation in esperite at high temperature, which involves the development of a hexagonal array of stacking faults when a single crystal is quenched from ~710 °C.

As to why our sample 2 is twinned and sample 1 is not, a probable explanation is as follows. Due to the slight chemical difference between the two samples (Table 5), the highest metamorphic temperature (T_{HM}) that our sample had reached during its formation might be just high enough for sample 2, but not high enough for sample 1, to undergo the transformation process to the high-temperature form detected by Moore and Ribbe (1965). Since esperite starts to decompose to hardystonite + larsenite + zincite between 700 and 800 °C, depending on its chemical composition (Moore and Ribbe 1965; Ito 1968), we estimate the T_{HM} value that our sample reached to be ~700 °C. This temperature is in good agreement with that (720 to 750 °C) estimated by many previous studies for the metamorphosed marine-exhalative deposits in Franklin, New Jersey (e.g., Mason 1947; Hewins and Yersak 1977; Carvalho and Sclar 1988; Sclar 1990; Leavens and Nelen 1990; Moore et al. 2003). If the argument we presented above holds true, then the twinning in esperite, despite the rarity of the mineral, may serve as a potential geothermometer.

ACKNOWLEDGMENTS

The authors gratefully acknowledge support for this study from the RRUFF project, the NSF grant EAR-0609906, and the Canadian Museum of Nature Mineral Collection for providing the sample (CMNMC 56855). Constructive comments from A. Guastoni, R. Peterson, and an anonymous reviewer are appreciated.

REFERENCES CITED

Abel, E.W. (1973) Lead. In A.F. Trotman-Dickinson, Ed., Comprehensive Inorganic Chemistry, p. 105–146. Pergamon Press, Oxford.

Aminoff, G. (1926) Zur kristallographie des trimerits. Geologiska Föreningens i Stockholm Förhandlingar, 48, 19–43.

Barbier, J. and Fleet, M.E. (1987) Investigation of structural states in the series MGaSiO$_4$, MAlGeO$_4$, MGaGeO$_4$ (M = Na, K). Journal of Solid State Chemistry, 71, 361–370.

——— (1988) Investigation of phase relations in the (Na,K)AlGeO$_4$ system. Physics and Chemistry of Minerals, 16, 276–285.

Brese, N.E. and O'Keeffe, M. (1991) Bond-valence parameters for solids. Acta Crystallographica, B47, 192–197.

Carvalho III, A.V. and Sclar, C.B. (1988) Experimental determination of the ZnFe$_2$O$_4$-ZnAl$_2$O$_4$ miscibility gap with applications to franklinite-gahnite exsolution intergrowths from the Sterling Hill zinc deposit, New Jersey. Economical Geology, 83, 1447–1452.

Chen, S., Fleet, M.E., and Pan, Y. (1994) Phase relations in the system NaAlSiO$_4$-NaGaSiO$_4$. Physics and Chemistry of Minerals, 20, 594–600.

Downs, R.T., Hazen, R.M., and Finger, L.W. (1995) Crystal chemistry of lead aluminosilicate hollandite: A new high-pressure synthetic phase with octahedral Si. American Mineralogist, 80, 937–940.

Dunn, P.J. (1985) The lead silicates from Franklin, New Jersey: Occurrence and composition. Mineralogical Magazine, 49, 721–727.

Giuseppetti, G. and Tadini, C. (1973) Refinement of the crystal structure of beryllonite, NaBePO$_4$. Tschermaks Mineralogishe und Petrographische Mitteilungen, 20, 1–12.

Golovastikov, N.I. (1961) The crystal structure of beryllonite (NaBePO$_4$). Soviet Physics. Crystallography, 6, 733–739.

Graetsch, H.A. and Schreyer, W. (2005) Rietveld refinement of synthetic monoclinic NaBSiO$_4$. Canadian Mineralogist, 43, 759–767.

Grundmann, G., Lehrberger, G., and Schnorrer-Köhler, G. (1990) The El Dragón Mine, Potosí Bolivia. Mineralogical Record, 21, 142.

Hammond, R., Barbier, J., and Gallardo, C. (1998) Crystal structures and crystal chemistry of AgXPO$_4$ (X = Be, Zn). Journal of Solid State Chemistry, 141, 177–185.

Henderson, C.M.B. and Roux, J. (1977) Inversions in sub-potassic nephelines. Contributions to Mineralogy and Petrology, 61, 279–298.

Hewins, R.H. and Yersak, T.E. (1977) Conditions of the formation of the Franklin-Sterling ores, New Jersey. Geological Association of Canada Program with Abstracts, 2, 24.

Hill, R.J. (1985) Refinement of the structure of orthorhombic PbO (massicot) by Rietveld analysis of neutron powder diffraction data. Acta Crystallographica, C41, 1281–1284.

Hörkner, W. and Müller-Buschbaum, H.K. (1976) Zur kristallstruktur von CaAl$_2$O$_4$. Journal of Inorganic and Nuclear Chemistry, 38, 983–984.

Iijima, K., Marumo, F., and Takei, H. (1982) The room-temperature structure of BaZnGeO$_4$. Acta Crystallographica, B38, 1112–1116.

Ito, J. (1968) Synthesis of some lead calcium zinc silicates. American Mineralogist, 53, 231–240.

Kahlenberg, V. (2001) On the Al/Fe substitution in iron doped monocalcium aluminate—The crystal structure of CaAl$_{1.8}$Fe$_{0.2}$O$_4$. European Journal of Mineralogy, 13, 403–410.

Khavryuchenko, V.D., Khavryuchenko, O.V., and Lisnyak, V.V. (2007) Quantum chemical insight on vibration spectra of silica systems. Molecular Simulation, 33, 531–540.

Kihara, K., Hirose, T., and Shinoda, K. (2005) Raman spectra, normal modes and disorder in monoclinic tridymite and its higher temperature orthorhombic modification. Journal of Mineralogical and Petrological Sciences, 100, 91–103.

Klaska, K.H. and Jarchow, O. (1977) Die bestimmung der kristallstruktur von trimerite CaMn$_2$(BeSiO$_4$)$_3$ und das trimeritgesetz der verzwillingung. Zietschrift für Krystallographie und Mineralogie, 145, 46–65.

Klaska, R., Klaska, K.-H., and Jarchow, O. (1979) Struktur und verwachsung zweie topologisch unterschiedlicher tetraedergerüste der pseudosymmetric *Icmm*. Zeitschrift für Kristallographie, 149, 135–136.

Layman, F.G. (1957) Unit cell and space group of larsenite, PbZnSiO$_4$. American Mineralogist, 42, 910–911.

Leavens, P.B. and Nelen, J.A. (1990) Franklinites from Franklin and Sterling Hill, New Jersey and oxygen fugacities of the deposits. Symposium on Character and Origin of the Franklin-Sterling Hill Orebodies, Lehigh University, Proceedings Volume, 49–62.

Liu, B. and Barbier, J. (1993) Structures of the stuffed tridymite derivatives, BaM-SiO$_4$ (M = Co, Zn, Mg). Journal of Solid State Chemistry, 102, 115–125.

Mason, B.M. (1947) Mineralogical aspects of the system Fe$_3$O$_4$-Mn$_3$O$_4$-ZnMn$_2$O$_4$-ZnFe$_2$O$_4$. American Mineralogist, 32, 426–441.

Moore, A.D., Leavens, P.B., Jenkins II, R.E., and Altounian, N.M. (2003) Wollastonite at the Sterling Hill Fe-Zn-Mn ore body, Ogdensburg, New Jersey. Mineralogy and Petrology, 79, 225–241.

Moore, P.B. and Ribbe, P.H. (1965) A study of "calcium-larsenite" renamed esperite. American Mineralogist, 50, 1170–1178.

Palache, C. (1935) The Minerals of Franklin and Sterling Hill, Sussex County, New Jersey. U.S. Geological Survey Professional Paper 180, p. 80–81.

Palache, G., Bauer, L.H., and Berman, H. (1928a) Larsenite and calcium-larsenite, new members of the crystolite group, from Franklin, New Jersey. American Mineralogist, 13, 142–144.

——— (1928b) Larsenite, calcium larsenite, and the associated minerals at Franklin, New Jersey. American Mineralogist, 13, 334–340.

Sahl, K. (1970) Lead. 82-A. Crystal Chemistry. In K.H. Wedepohl, Ed., Handbook of Geochemistry II-5, p. 821–826. Springer-Verlag, Berlin.

Sandomirskii, P.A., Meshalkin, S.S., Rozhdestvenskaya, I.V., Dem'yanets, L.N., and Uvarova, T.G. (1986) Crystal structures of the D-phase of KAlGeO$_4$ and the C-phase of NaAlGeO$_4$. Kristallografiya, 31, 522–527.

Sclar, G.B. (1990) Geothermometry at the Sterling Hill zinc deposit, Sussex County, New Jersey (just how hot did it get at Sterling Hill?). Symposium on Character and Origin of the Franklin-Sterling Hill Orebodies, Lehigh University, Proceedings Volume, p. 110–118.

Sheldrick, G.M. (1997) The SHELX-97 Manual. University of Göttingen, Germany.

——— (2007) TWINABS. University of Göttingen, Germany.

——— (2008) A short history of SHELX. Acta Crystallographica, A64, 112–122.

Sokolova, E.V., Hawthorne, F.C., and Khomyakov, A.P. (2001) The crystal chemistry of malinkoite, NaBSiO$_4$, and lisitsynite, KBSi$_2$O$_6$, from the Khibina-Lovozero complex, Kola Peninsula, Russia. Canadian Mineralogist, 39, 159–169.

Swainson, I.P., Dove, M.T., and Palmer, D.C. (2003) Infrared and Raman spectroscopy studies of the - phase transition in cristobalite. Physics and Chemistry of Minerals, 30, 353–365.

Taylor, D. (1983) The structural behavior of tetrahedral framework compounds—a review. Part I. Structural behavior. Mineralogical Magazine, 47, 319–326.

——— (1984) The structural behavior of tetrahedral framework compounds—a review. Part II. Framework structures. Mineralogical Magazine, 48, 65–79.

Yang, H. and Downs, R.T. (2008) Crystal structure of glaucodot, (Co,Fe)AsS, and its relationships to marcasite and arsenopyrite. American Mineralogist, 93, 1183–1186.

Zhang, M., Xu, H., Salje, E.K.H., and Heaney, P.J. (2003) Vibrational spectroscopy of beta-eucryptite (LiAlSiO$_4$): optical phonons and phase transition(s). Physics and Chemistry of Minerals, 30, 457–462.

MANUSCRIPT RECEIVED OCTOBER 2, 2009
MANUSCRIPT ACCEPTED DECEMBER 15, 2009
MANUSCRIPT HANDLED BY G. DIEGO GATTA